Supporting Information for

Encapsulating porous SnO_2 into hybrid nanocarbon matrix for long lifetime Li storage

Yi Zhao,[ab] Luyuan Paul Wang,[bd] Shibo Xi,[c] Yonghua Du,[c] Qianqian Yao,[a] Lunhui Guan, *[a] Zhichuan J. Xu*[bde]

[a]CAS Key Laboratory of Design and Assembly of Functional Nanostructures, and Fujian Key Laboratory of Nanomaterials, Fujian Institute of Research on the Structure of Matter, Chinese Academy of Sciences. Fuzhou 350108, China

[b]School of Materials Science and Engineering, Nanyang Technological University, Singapore 639798, Singapore

[c]Institute of Chemical and Engineering Sciences A*STAR, 1 Pesek Road, 627833, Singapore

[d]Singapore-HUJ Alliance for Research and Enterprise (SHARE), Nanomaterials for Energy and Energy-Water Nexus (NEW), Campus for Research Excellence and Technological Enterprise (CREATE), Singapore 138602

[e]Energy Research Institute @ NTU, Nanyang Technological University, 50 Nanyang Drive, Singapore, Singapore 639798, Singapore

*Corresponding Author

E-mail: xuzc@ntu.edu.sg, guanlh@fjirsm.ac.cn

EXPERIMENTAL SECTION

Synthesis of G@porous SiO_2 composite: The graphene oxide (GO) was synthesized via a modified Hummer's method. In a typical experiment, 160 mg cetyltrimethylammonium bromide (CTAB) was firstly dissolved in a mixture of 30 ml H_2O, 120 ml ethanol, and 1.5 ml $NH_3.H_2O$. Then, 40 mg GO was dispersed in the above solution by ultrasonication, followed with slow addition of 1 mL tetraethyl orthosilicate (TEOS) and kept under stirring for 12 h. After washed with H_2O and dried at 80 ^oC, this product was further annealing at 800 ^oC for 3 h at Ar atmosphere to obtain G@porous SiO_2 composite.

Synthesis of G@SiO_2@SnO_2 composite: 200 mg G@porous SiO_2 composite and 250 mg $SnCl_2.2H_2O$ was firstly dispersed into 10 ml ethanol by ultrasonication. Then, the above solution was stirred at 45 ^oC to evaporate the ethanol. The obtained mixture was fine ground and calcinated at 350 ^oC for 3h in Air to obtain G@SiO_2@SnO_2 composite.

Synthesis of G@p-SnO_2@C composite: Typically, 160 mg above G@SiO_2@SnO_2 composite was sonicated in 14 mL H_2O for 0.5 h. Then, 0.05 mL $NH_3.H_2O$ and 0.5 ml 0.01 M CTAB aqueous solutions were dropped into the above dispersion. After vigorously stirred for 0.5 h, 25 mg resorcinol and 35µl formaldehyde were added and kept under stirring for 16 h at room temperature. The obtained product was filtered and washed with water, dried at 80 ^oC, and calcinated at 600 ^oC for 2 h under Ar atmosphere for carbonization. Finally, SiO_2 layer was

removed with 1M NaOH solution at 50 ^{o}C for 12 h to obtain G@p-SnO_2@C composite. The G@p-SnO_2 composite was fabricated by directly etching the G@SiO_2@SnO_2 composite with 1M NaOH solution.

Synthesis of G@SnO_2 and G@SnO_2@C composites: G@SnO_2 composite was synthesized through the redox reaction between GO and $SnCl_2$. In a typical experiment, 200 mg $SnCl_2$ was added into 50 mL 0.2 HCl solution containing 24 mg GO. After being stirred for 1 h at room temperature, this solution was further refluxed at 90 ^{o}C for 1 h to obtain G@SnO_2 composite. For the synthesis of G@SnO_2@C composite, 50 mg G@SnO_2 was added into 7 ml 0.25M glucose solution and sonicated for 0.5 h. Then, the solution was transferred into 25 mL Teflon-line stainless steel autoclave and kept at 170 ^{o}C for 3 h. After filtered and washed with ethanol and water, this sample was annealed at 500 ^{o}C for 3h at Ar atmosphere to obtain G@SnO_2@C composite.

Materials Characterization: The structure and morphology of the obtained samples were characterized via scanning electron microscopy (SEM, JSM-7600F and SU-8010), transmission electron microscope (TEM, JEM-2010F and Tecnai F20), x-ray photoelectron spectroscopy (XPS, ESCALAB 250Xi), Brunauer–Emmett–Teller surface area analyzer (BET, Micromeritics ASAP2020), X-ray diffraction (Shimadzu, XRD-6000), and Thermogravimetry analyses (TGA, Q500). XANES was performed at Singapore Synchrotron Light Source, XAFCA beamline.

Electrochemical Measurements: The electrochemical behaviors of G@p-

SnO_2@C and G@p-SnO_2 composites were investigated via CR2032 coin-type test cells. The working electrodes consisted of 80 wt% active materials, 10 wt% conductive carbon (ketjen black), and 10 wt% carboxymethyl cellulose as the binder, which were mixed with de-ionized water, pasted on Ni foam, and then dried at 80 ^{o}C overnight under vacuum before use. Cells were assembled in an Ar-filled glove box with concentration of moisture and oxygen below 1 ppm. The counter electrode was lithium foil and the separator was celgard 2300 membrane. The electrolyte was 1M $LiPF_6$ in ethylene carbonate (EC): ethylmethyl carbonate (EMC): dimethyl carbonate (DMC) with a volume ratio of 1: 1: 1. The obtained cells were discharged and charged on a Neware Battery tester over a range of 0.05 V to 3.0 V vs. Li^+/Li at room temperature. Cyclic voltammetry (CV) test was carried out on a PINE WaveDriver 20 bipotentiostat with a scan rate of 0.5 mV s^{-1}.

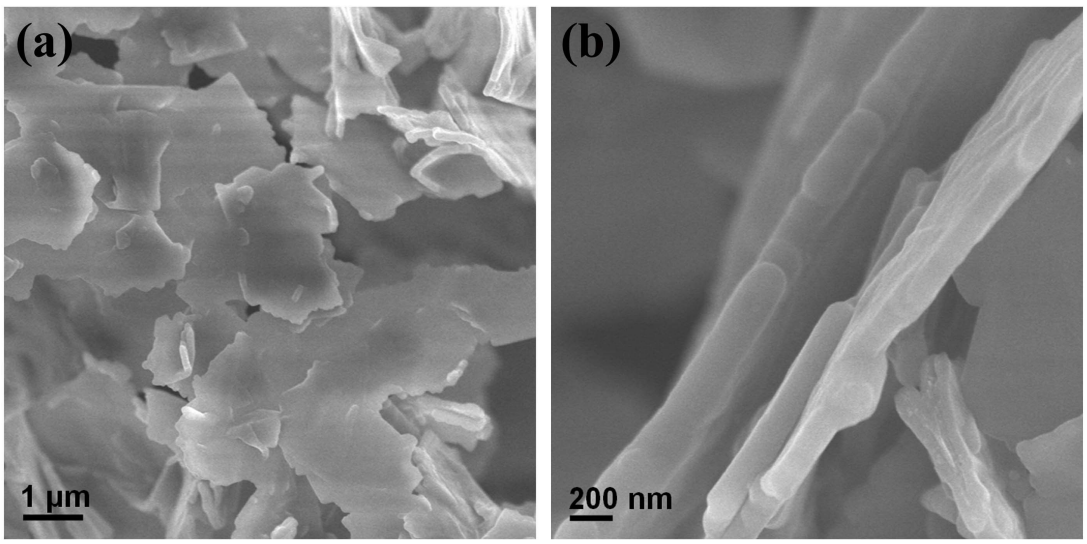

Fig. S1 (a-b) SEM images of G@porous SiO_2 composite.

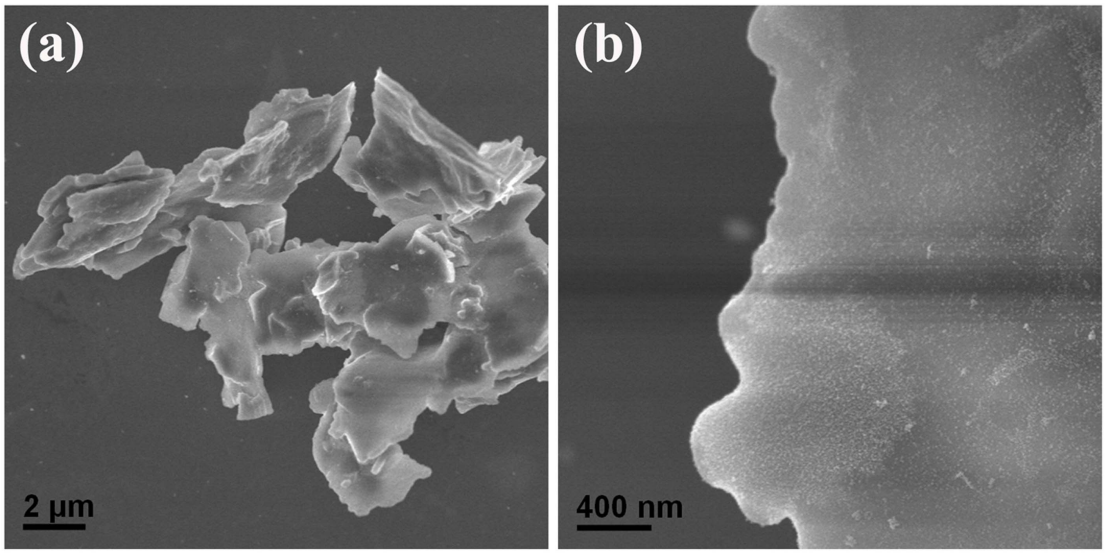

Fig. S2 (a-b) SEM images of G@SiO_2@SnO_2 composite.

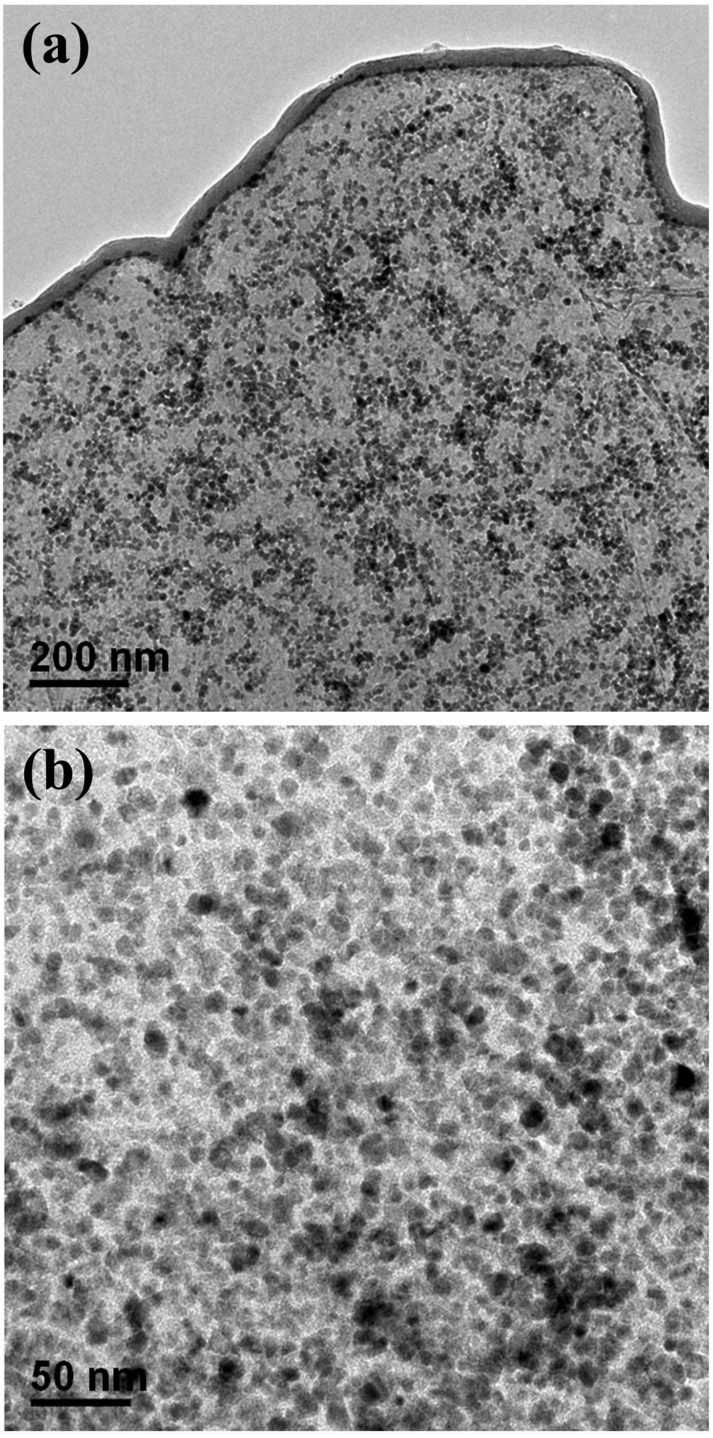

Fig. S3 (a-b) TEM images of G@p-SnO_2@C composite from other aspect.

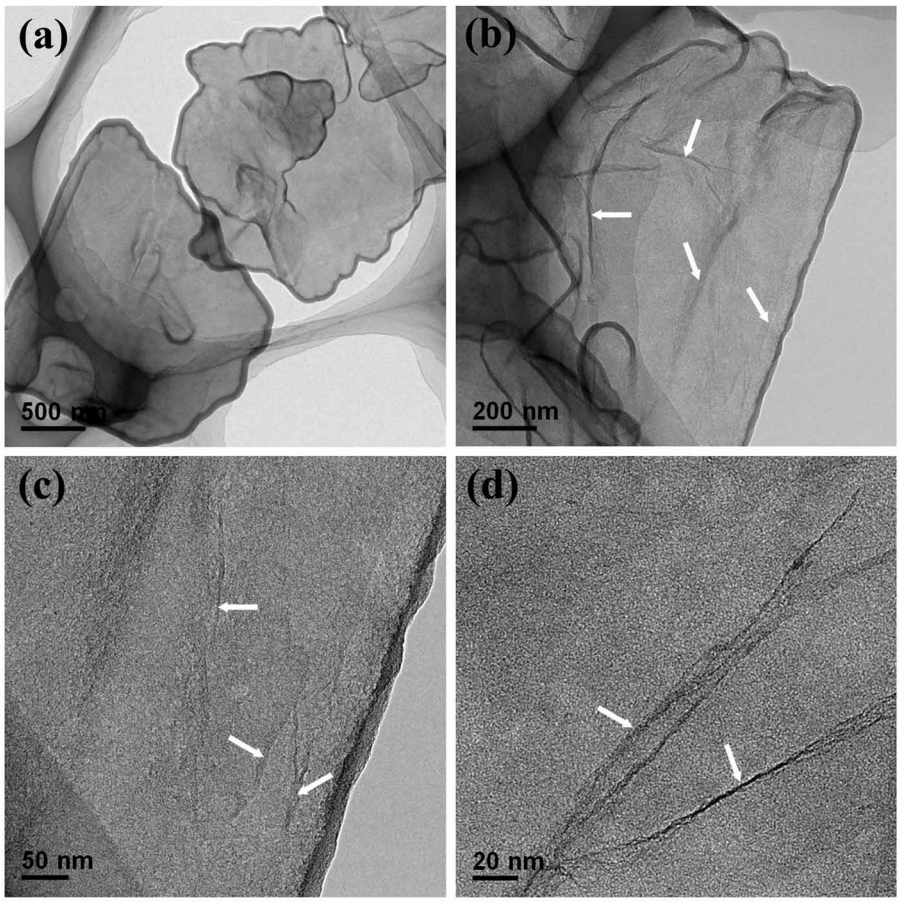

Fig. S4 TEM images of the pure hybrid nanocarbon matrix, showing the "carbon house" microstructure of this composite with graphene (white arrows) as "floor" and carbon coating layer as "walls and ceiling".

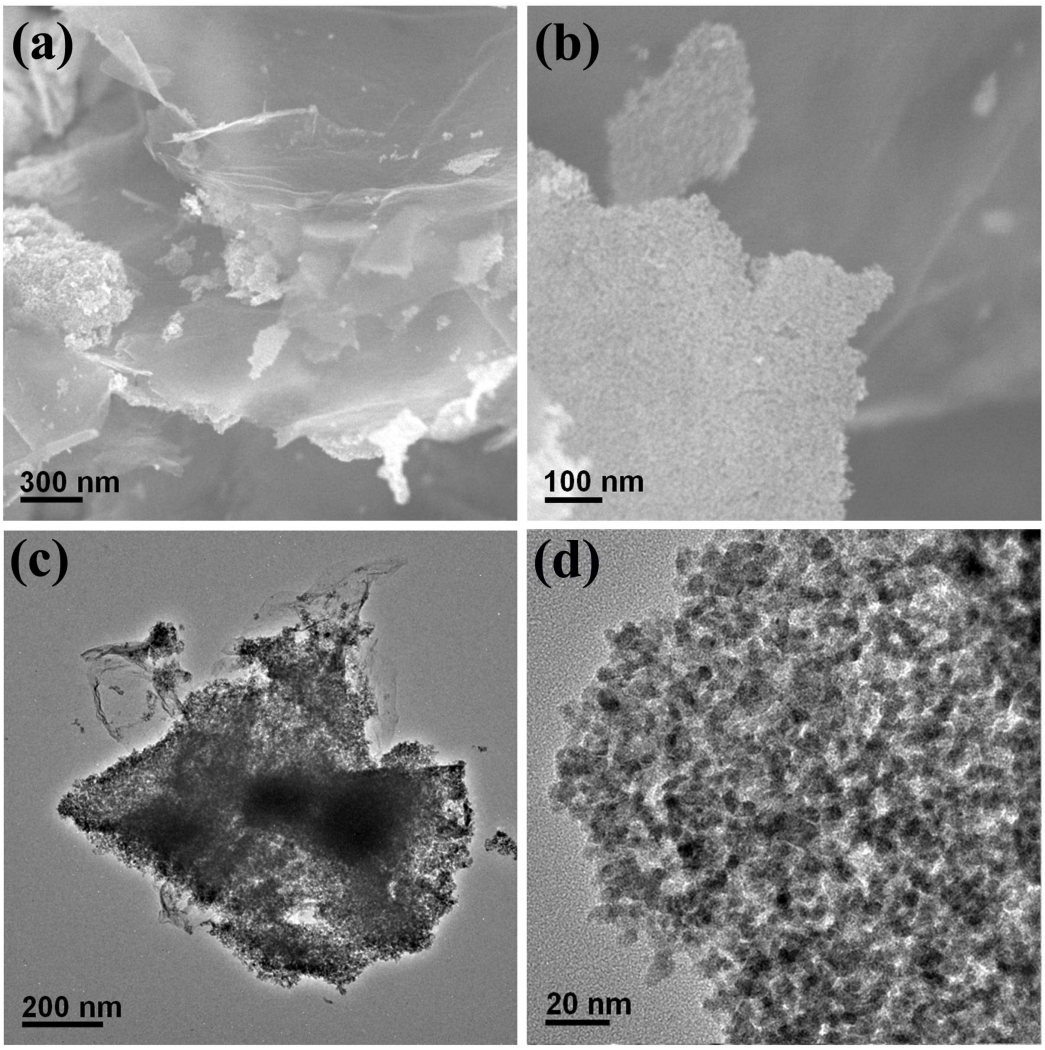

Fig. S5 (a-b) SEM and (c-d) TEM images of G@p-SnO_2.

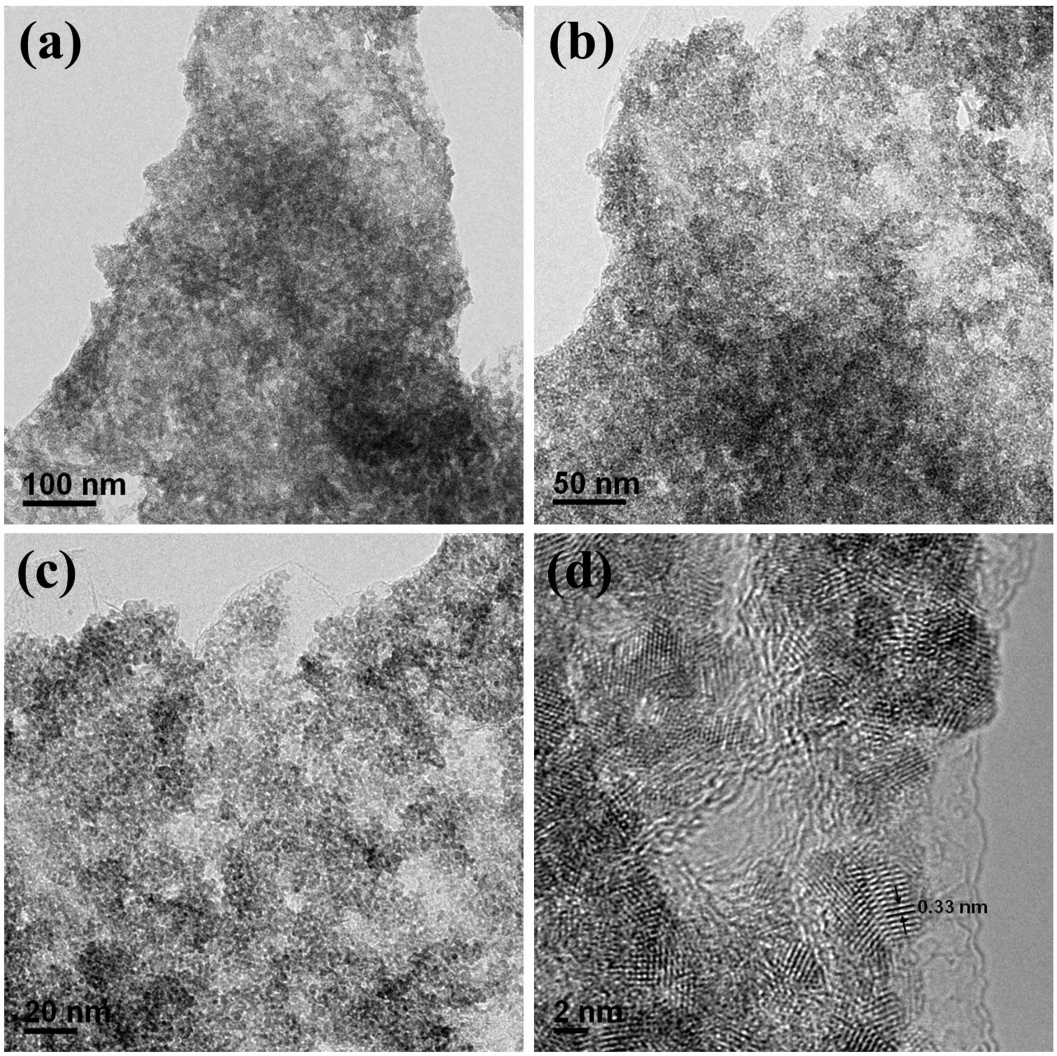

Fig. S6 TEM images of G@SnO_2 composite.

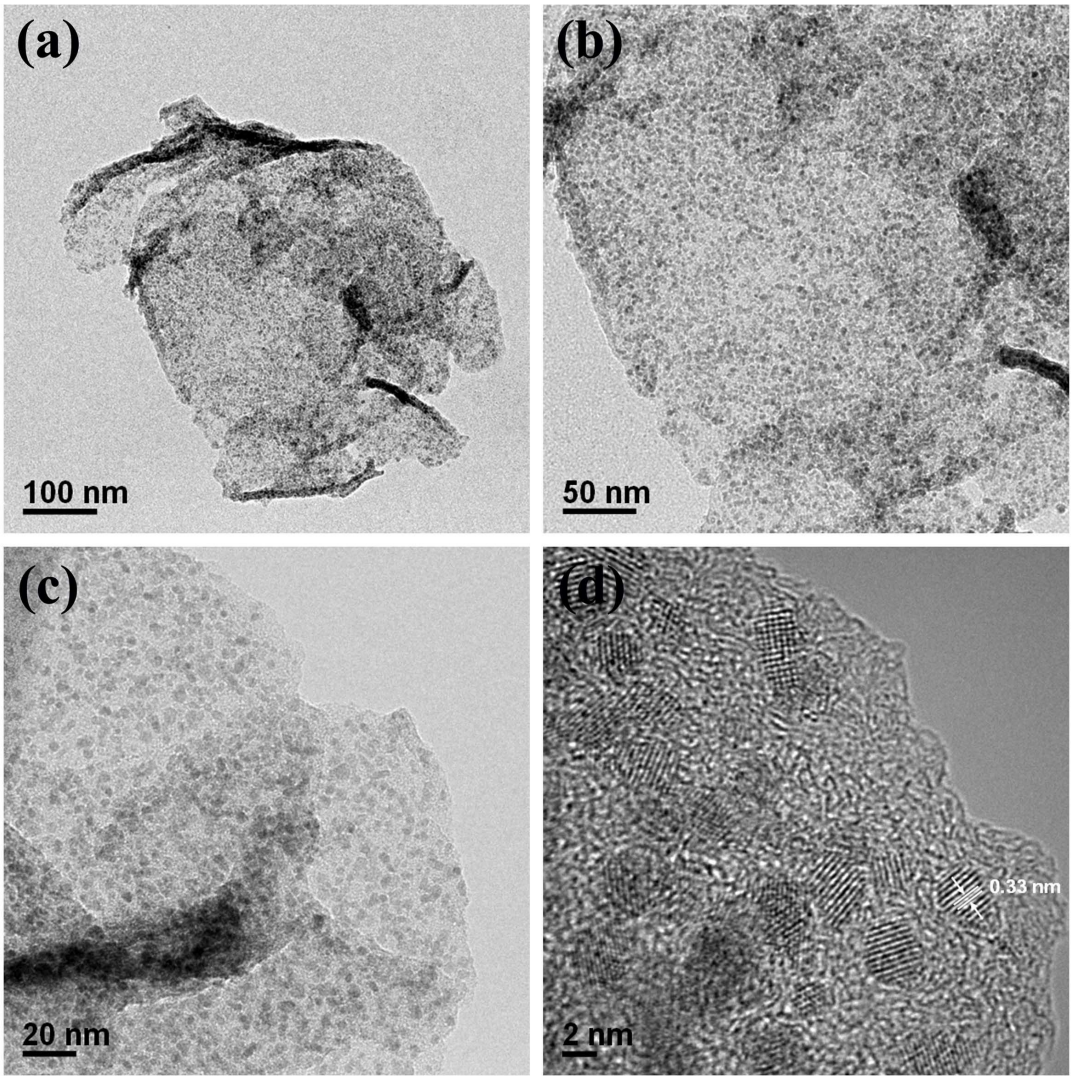

Fig. S7 TEM images of G@SnO_2@C composite.

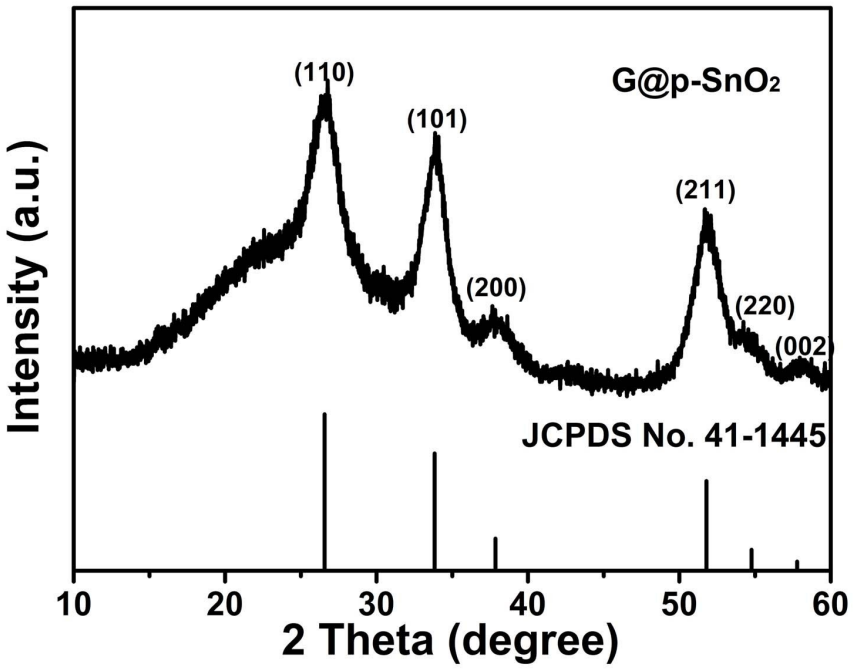

Fig. S8 XRD pattern of G@p-SnO_2 composite.

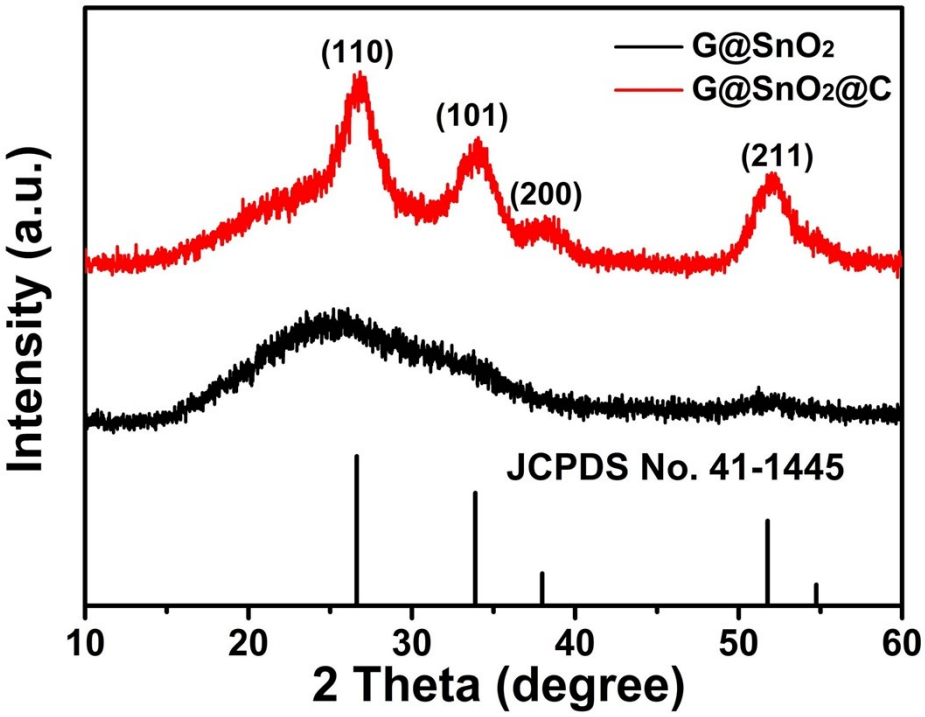

Fig. S9 XRD patterns of G@SnO_2 and G@SnO_2@C composites.

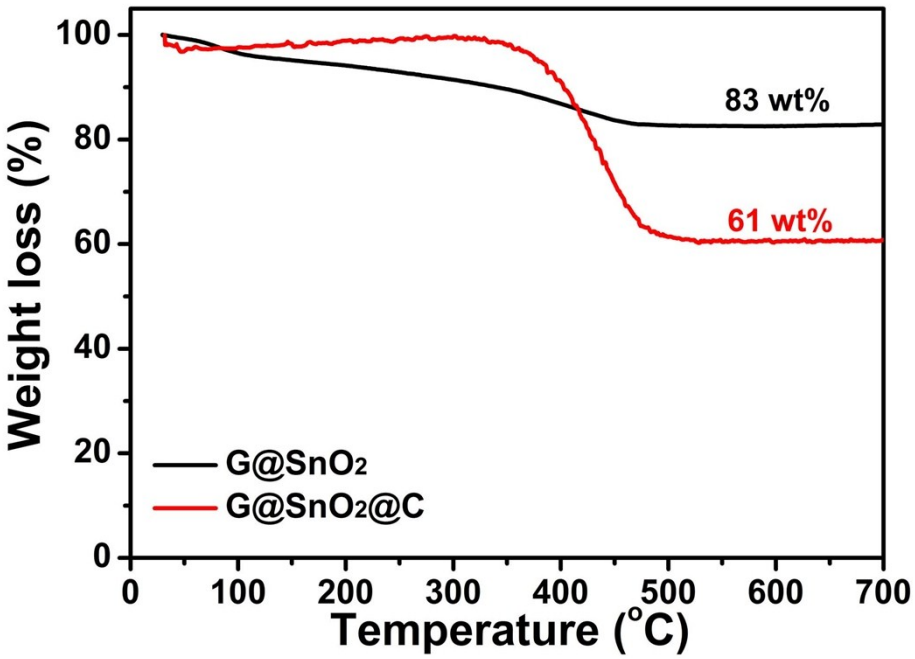

Fig. S10 TGA curves of G@SnO_2 and G@SnO_2@C composites.

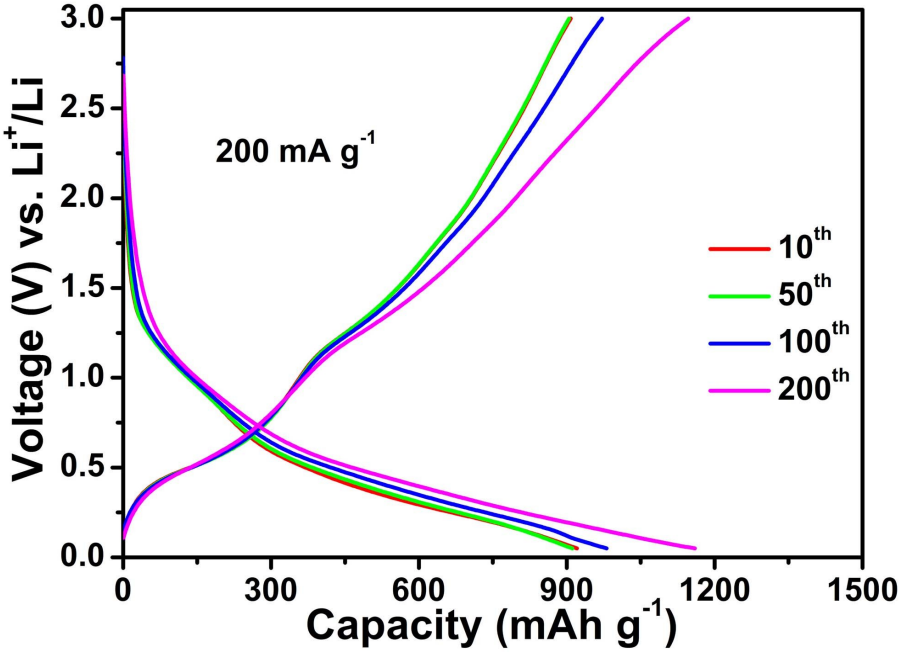

Fig. S11 Selected discharge/charge profiles of G@p-SnO_2@C electrode at 200 mA g^{-1} for LIBs.

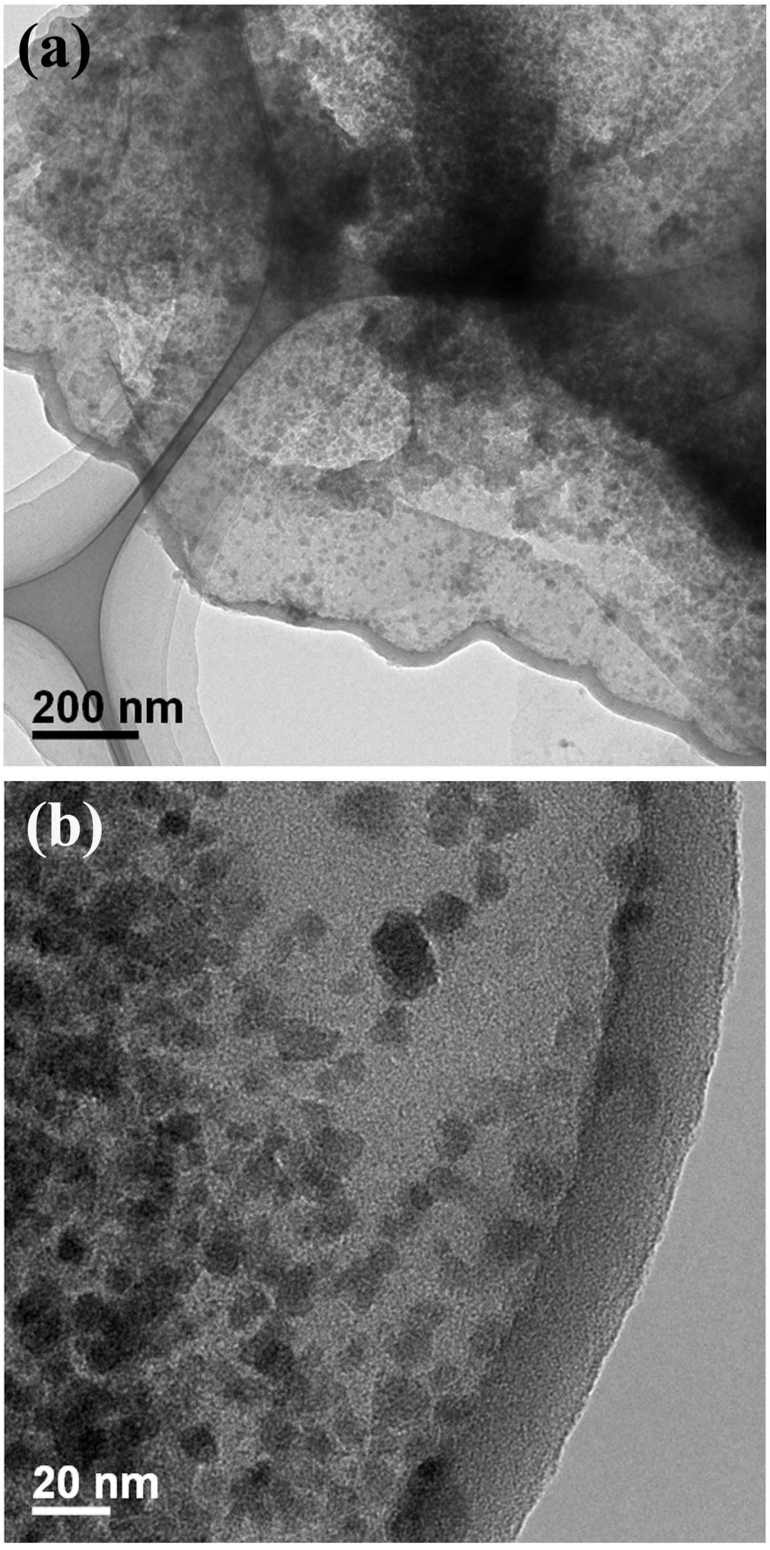

Fig. S12 (a-b) TEM images of G@p-SnO_2@C electrode after first discharge-charge cycle for LIBs.

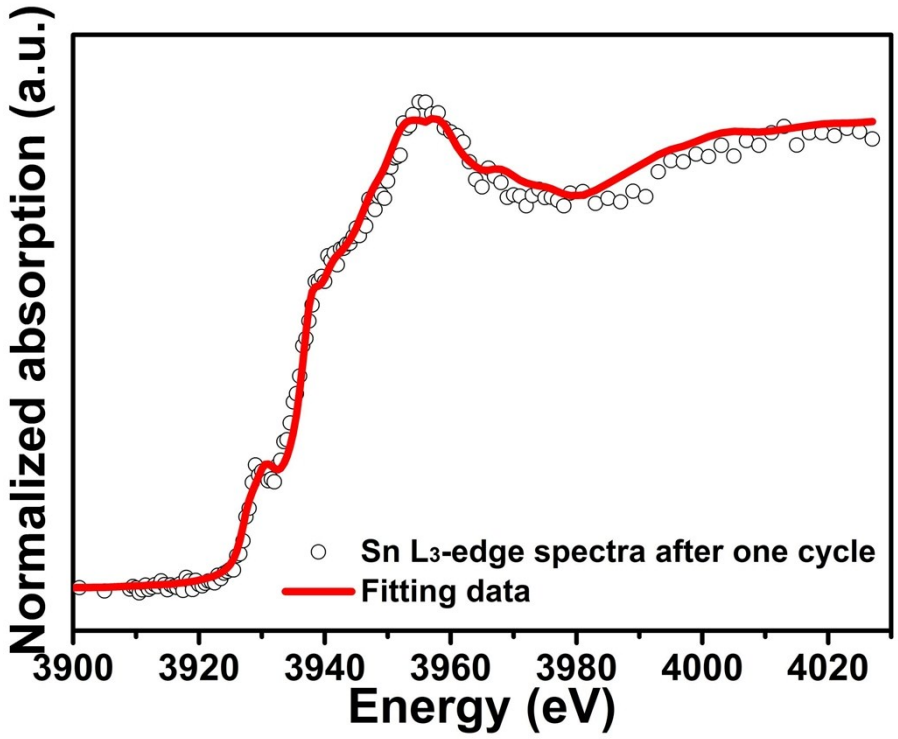

Fig. S13 The Sn L_3-edge XANES spectra of G@p-SnO_2@C electrode and its fitting data based on linear combination fit analysis with commercial SnO_2 and SnO as standards.

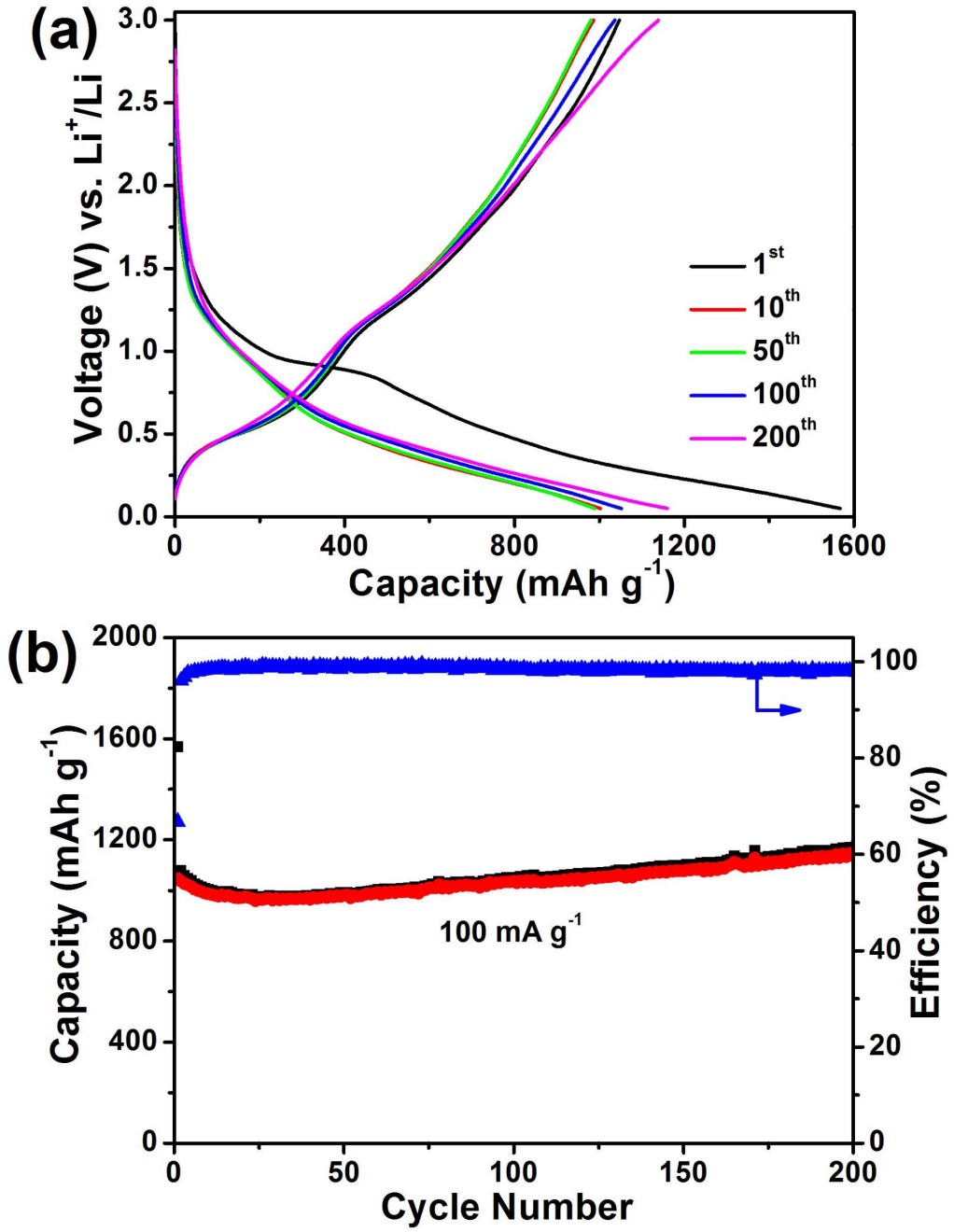

Fig. S14 (a) Typical discharge/charge profiles, and (b) cycling performance of G@p-SnO_2@C electrode at 100 mA g^{-1} for LIBs.

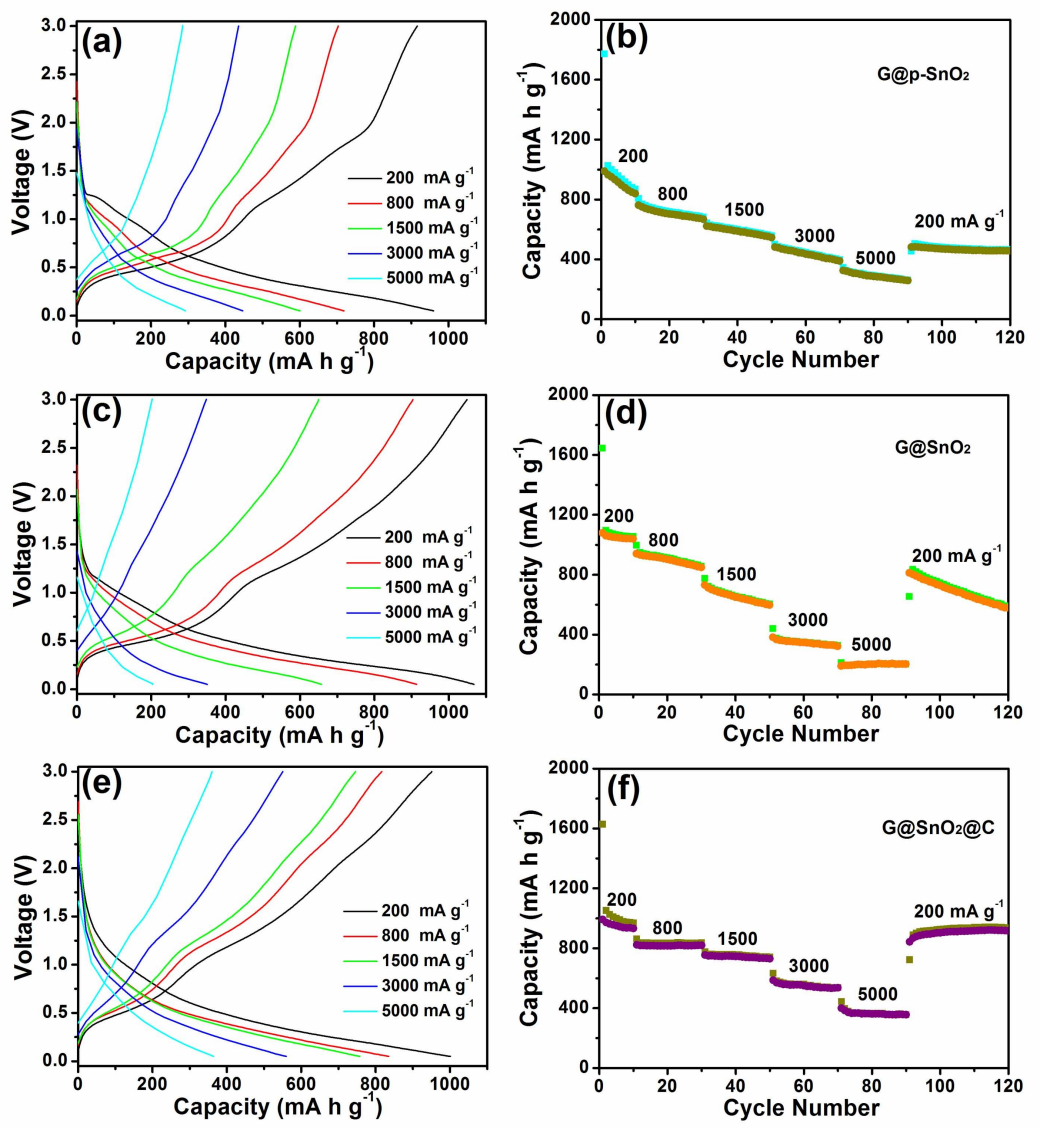

Fig. S15 (a, c, e) Discharge and charge profiles at various current densities and (b, d, f) rate performance of (a-b) G@p-SnO_2, (c-d) G@SnO_2, and (e-f) G@SnO_2@C composites.

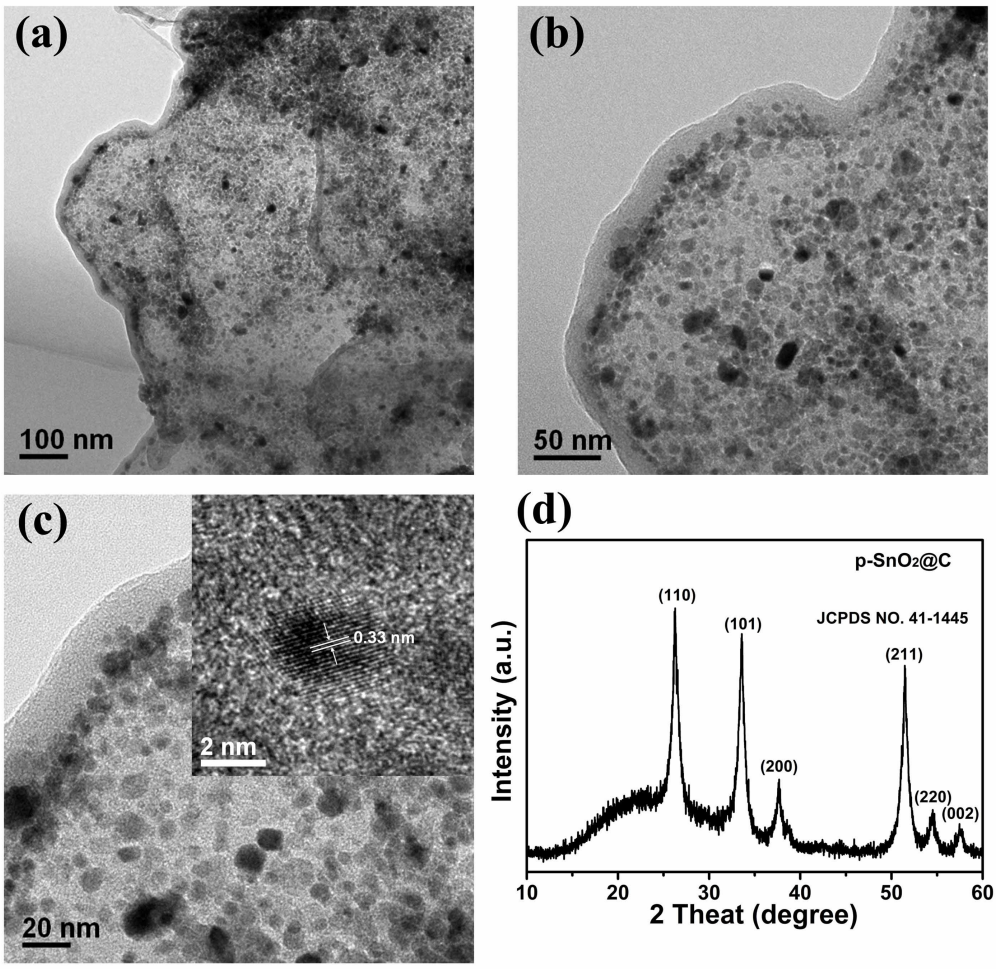

Fig. S16 (a-c) TEM images of p-SnO_2@C composite under various magnifications. Inset in (c) is the HRTEM image of SnO_2 NPs. (d) XRD pattern of p-SnO_2@C composite.

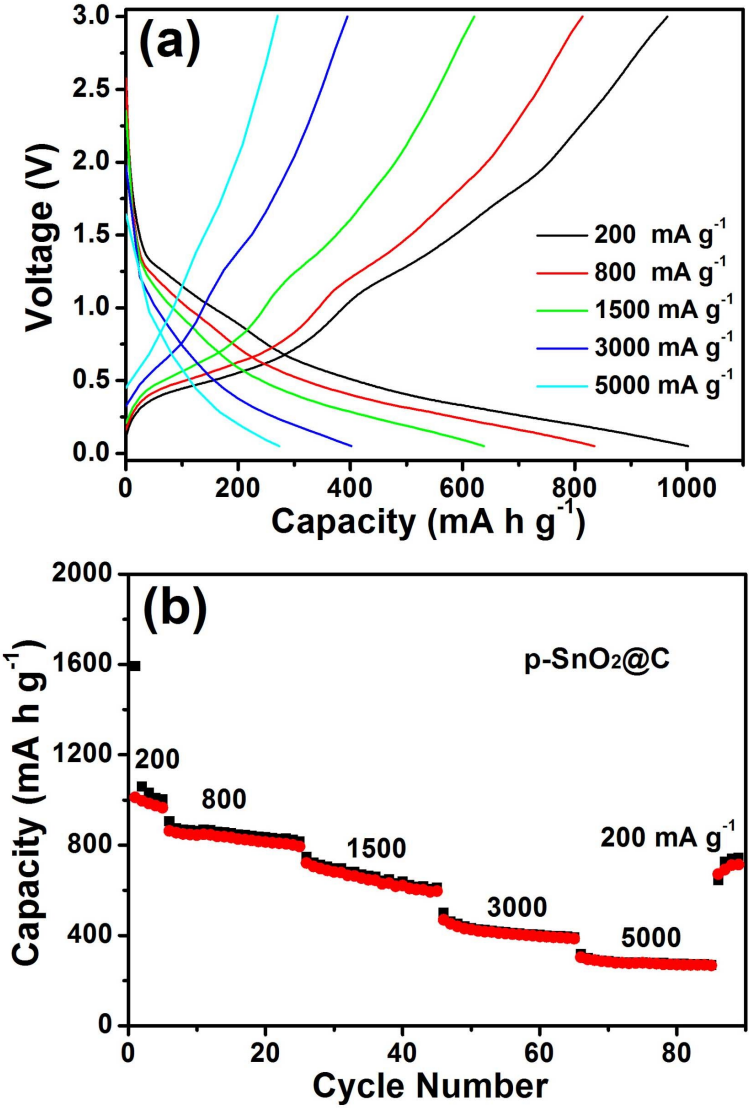

Fig. S17 (a) Discharge and charge profiles and (b) rate performance of p-SnO_2@C composite at various current densities. At high rate of 1.5, 3, and 5.0 A g^{-1}, p-SnO_2@C only delivered rate capabilities of 630, 400, and 270 mA h g^{-1}, much lower than the values of G@p-SnO_2@C. This result demonstrated that the existence of rGO can significantly enhance the rate performance of G@p-SnO_2@C composite, probably due to the effect of rGO to improve both the electron and Li^+ ion transport and shorten their diffusion length.

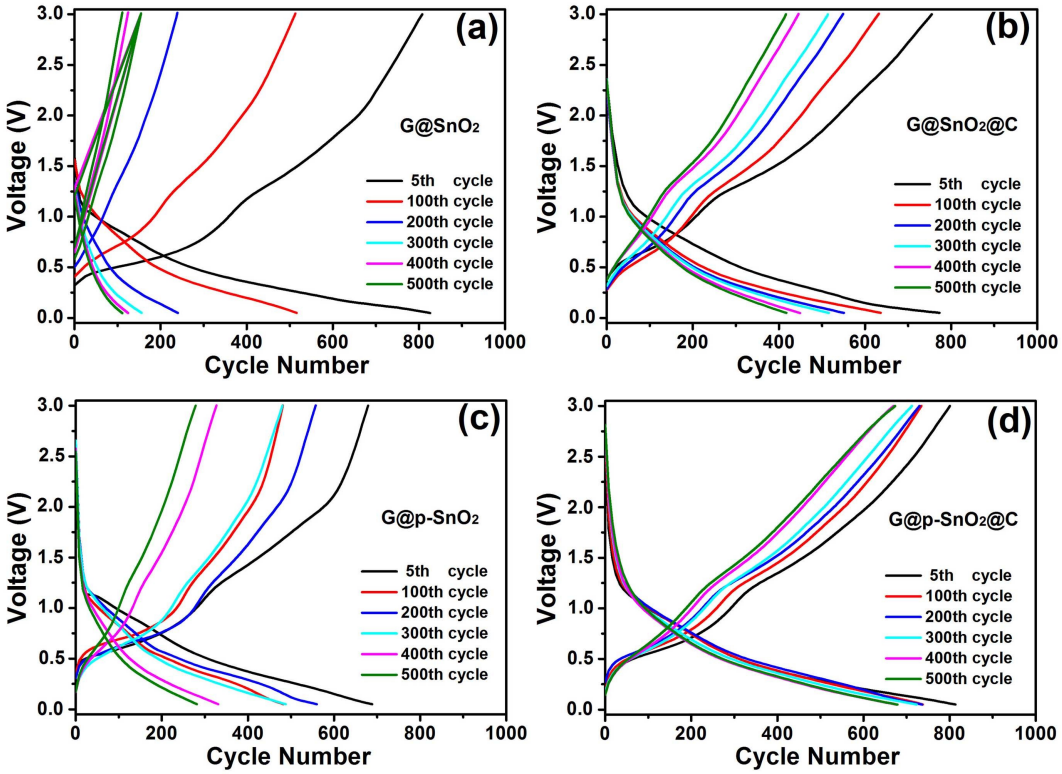

Fig. S18 Typical discharge-charge profiles of (a) G@SnO_2, (b) G@SnO_2@C, (c) G@p-SnO_2, and (d) G@p-SnO_2@C composites at 1.5 A g^{-1}.

Table S1. Electrochemical performance of SnO_2-based anode materials for LIBs.

Materials	Current density (mA g^{-1})	**Cycle Number**	Capacity (mAh g^{-1})	Loading of active material (mg cm^{-2})	Reference
Nanostructured SnO_2 anodes					
SnO_2 nanowires	100	**50**	~230	-	[1]
Hollow SnO_2 sphere	160	**20**	~650	-	[2]
SnO_2 nanotube	100	**30**	468	-	[3]
SnO_2 nanoboxes	0.2 C	**40**	570	-	[4]
Interconnected SnO_2 NPs	1500	**100**	430	-	[5]
SnO_2-in-TiO_2 wire-in-tube	400	**1000**	393	4.15	[6]
SnO_2/NiO nanotube@Ag	1000	**500**	826	3	[7]
SnO_2 hollow microsphere	100	**50**	750	1	[8]
SnO_2-carbon based anodes					
Hollow SnO_2@C	500	**100**	460	1.5	[9]
SnO_2@C nanotube	200	**50**	700	-	[10]
SnO_2@C microboxes	200	**150**	550	-	[11]
SnO_2@C nanotube	500	**200**	596	-	[12]
SnO_2@C	100	**200**	880	-	[13]
Hollow SnO_2@N-C box	500	**100**	491	1.5	[14]
SnO_2 in porous carbon	1000	**800**	930	0.7-1	[15]
SnO_2@N-carbon nanofiber	1000	**300**	754	-	[16]
Yolk-shell SnO_2@C	1C	**300**	516	0.6-1.0	[17]
SnO_2@C nanotube	500	**100**	663	-	[18]
Hollow SnO_2@C microsphere	500	**100**	600	-	[19]
SnO_2@C	200	**550**	649	-	[20]

Pipe-Wire TiO_2−Sn@CNF	200	**1100**	643	-	[21]
SnO_2-polydopamine coating	160	**300**	1300	-	[22]
SnO_2-Mn-graphite	1000	**900**	600	1.0-1.5	[23]
Graphene-SnO_2 based anodes					
Graphene@SnO_2	50	**30**	570	-	[24]
N-doped G@SnO_2	50	**50**	910	-	[25]
G@porous SnO_2	78.2	**50**	847	-	[26]
N-doped G@SnO_2	500	**500**	1346	10	[27]
G@SnO_2@C	200	**100**	800	-	[28]
G@SnO_2 nanorod@C	1000	**330**	~770	-	[29]
G@SnO_2@C	100	**360**	1165	-	[30]
CNT@SnO_2@C	1000	**100**	1100	-	[31]
G@SnO_2-SnS@C	100	**110**	1236	-	[32]
Hollow SnO_2@G	1000	**500**	552	1.5-2.0	[33]
Graphene-SnO_{2-x}	200	**100**	950	-	[34]
Graphene-SnO_2	1000	**230**	970	3	[35]
Sb-SnO_2-CNT-graphene	1000	**1000**	685	1.2	[36]
G@p-SnO_2@G	**200** **1500**	**200** **1800**	**1146** **418**	**0.8-1.2**	**this work**

[1] M. S. Park, G. X. Wang, Y. M. Kang, D. Wexler, S. X. Dou, H. K. Liu, Angew. Chem. Int. Edit. **2007**, 46, 750.

[2] S. J. Ding, J. S. Chen, G. G. Qi, X. N. Duan, Z. Y. Wang, E. P. Giannelis, L. A. Archer, X. W. Lou, J. Am. Chem. Soc. **2011**, 133, 21.

[3] J. F. Ye, H. J. Zhang, R. Yang, X. G. Li, L. M. Qi, **Small** 2010, 6, 296.

[4] Z. Y. Wang, D. Y. Luan, F. Y. C. Boey, X. W. Lou, J. Am. Chem. Soc. **2011**, 133, 4738.

[5] V. Etacheri, G. A. Seisenbaeva, J. Caruthers, G. Daniel, J. M. Nedelec, V. G. Kessler, V. G. Pol, Adv. Energy Mater. **2015**, 5.

[6] C. Guan, X. H. Wang, Q. Zhang, Z. X. Fan, H. Zhang, H. J. Fan, Nano Lett. **2014**, 14, 4852.

[7] C. Kim, J. W. Jung, K. R. Yoon, D. Y. Youn, S. Park, I. D. Kim, Acs Nano **2016**, 10, 11317.

[8] J. Zhang, H. Ren, J. Y. Wang, J. Qi, R. B. Yu, D. Wang, Y. L. Liu, J. Mater. Chem. A **2016**, 4, 17673.

[9] X. W. Lou, C. M. Li, L. A. Archer, Adv. Mater. **2009**, 21, 2536.

[10] L. Zhang, G. Q. Zhang, H. B. Wu, L. Yu, X. W. Lou, Adv. Mater. **2013**, 25, 2589.

[11] L. Zhang, H. B. Wu, B. Liu, X. W. Lou, Energy Environ. Sci. **2014**, 7, 1013.

[12] X. S. Zhou, L. Yu, X. W. Lou, Nanoscale **2016**, 8, 8384.

[13] M. H. Wang, H. Yang, X. L. Zhou, W. Shi, Z. Zhou, P. Cheng, Chem. Commun. **2016**, 52, 717.

[14] X. S. Zhou, L. Yu, X. W. Lou, Adv. Energy Mater. **2016**, 6, 1600451.

[15] L. Shen, F. Liu, G. Chen, H. H. Zhou, Z. Y. Le, H. B. Wu, G. Wang, Y. F. Lu, J. Mater. Chem. A **2016**, 4, 18706.

[16] L. Xia, S. Q. Wang, G. X. Liu, L. X. Ding, D. D. Li, H. H. Wang, S. Z. Qiao, Small **2016**, 12, 853.

[17] B. Huang, X. H. Li, Y. Pei, S. Li, X. Cao, R. C. Masse, G. Z. Cao, Small **2016**, 12, 1945.

[18] C. H. Han, B. X. Zhang, K. N. Zhao, J. S. Meng, Q. He, P. He, W. Yang, Q. Li, L. Q. Mai, Chem. Commun. **2017**, 53, 9542.

[19] L. L. Hu, L. P. Yang, D. Zhang, X. S. Tao, C. Zeng, A. M. Cao, L. J. Wan, Chem. Commun. **2017**, 53, 11189.

[20] L. Y. Yang, S. T. Li, J. Liu, K. J. Zhu, S. L. Liu, M. Lei, J. Mater. Chem. A **2017**, 5, 1629.

[21] M. L. Mao, F. L. Yan, C. Y. Cui, J. M. Ma, M. Zhang, T. H. Wang, C. S. Wang,

Nano Lett. **2017**, 17, 3830.

[22] B. B. Jiang, Y. J. He, B. Li, S. Q. Zhao, S. Wang, Y. B. He, Z. Q. Lin, Angew. Chem. Int. Edit. **2017**, 56, 1869.

[23] R. Z. Hu, Y. P. Ouyang, T. Liang, X. Tang, B. Yuan, J. Liu, L. Zhang, L. C. Yang, M. Zhu, Energy Environ. Sci. **2017**, 10, 2017.

[24] S. M. Paek, E. Yoo, I. Honma, Nano Lett. **2009**, 9, 72.

[25] X. Wang, X. Q. Cao, L. Bourgeois, H. Guan, S. M. Chen, Y. T. Zhong, D. M. Tang, H. Q. Li, T. Y. Zhai, L. Li, Y. Bando, D. Golberg, Adv. Funct. Mater. **2012**, 22, 2682.

[26] S. Yang, W. B. Yue, J. Zhu, Y. Ren, X. J. Yang, Adv. Funct. Mater. **2013**, 23, 3570.

[27] X. S. Zhou, L. J. Wan, Y. G. Guo, Adv. Mater. **2013**, 25, 2152.

[28] Y. Z. Su, S. Li, D. Q. Wu, F. Zhang, H. W. Liang, P. F. Gao, C. Cheng, X. L. Feng, Acs Nano. **2012**, 6, 8349.

[29] D. N. Wang, J. L. Yang, X. F. Li, D. S. Geng, R. Y. Li, M. Cai, T. K. Sham, X. L. Sun, Energy Environ. Sci. **2013**, 6, 2900.

[30] Y. X. Liu, P. Liu, D. Q. Wu, Y. S. Huang, Y. P. Tang, Y. Z. Su, F. Zhang, X. L. Feng, Chem. Eur. J. **2015**, 21, 5617.

[31] C. R. Ma, W. M. Zhang, Y. S. He, Q. Gong, H. Y. Che, Z. F. Ma, Nanoscale **2016**, 8, 4121.

[32] J. Q. Shan, Y. X. Liu, P. Liu, Y. S. Huang, Y. Z. Su, D. Q. Wu, X. L. Feng, J. Mater. Chem. A **2015**, 3, 24148.

[33] X. Hu, G. Zeng, J. X. Chen, C. Z. Lu, Z. H. Wen, J. Mater. Chem. A **2017**, 5, 4535.

[34] W. J. Dong, J. J. Xu, C. Wang, Y. Lu, X. Y. Liu, X. Wang, X. T. Yuan, Z. Wang, T. Q. Lin, M. L. Sui, I. W. Chen, F. Q. Huang, Adv. Mater. **2017**, 29, 1700136.

[35] W. H. Chen, K. M. Song, L. W. Mi, X. M. Feng, J. M. Zhang, S. Z. Cui, C. T. Liu, J. Mater. Chem. A **2017**, 5, 10027.

[36] J. Cui, S. Yao, J.-Q. Huang, L. Qin, W. G. Chong, Z. Sadighi, J. Huang, Z. Wang, J.-K. Kim, Energy Storage Materials **2017**, 9, 85.

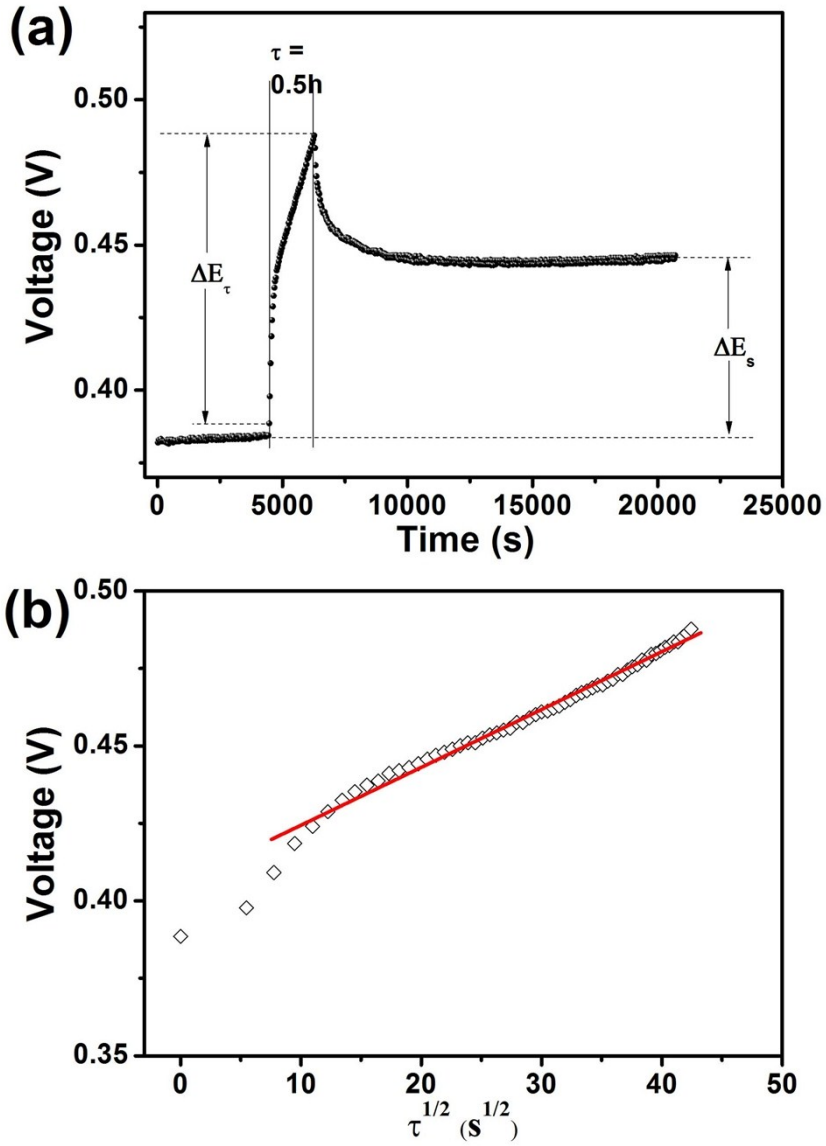

Fig. S19 (a) A single titration profile of G@p-SnO_2@C electrode during the third charge cycle with schematic illustration of different parameters. (b) Variation of voltage against $\tau^{1/2}$ to show the linear fit.

Table. S2 The fitting impedance parameters of G@p-SnO_2@C and G@p-SnO_2 electrodes after cycles.

electrodes	**cycles**	**R_s**	**R_{SEI}**	**R_{ct}**
G@p-SnO_2@C	3th	5.99	13.44	47.68
	100th	14.93	17.77	43.21
G@p-SnO_2	3th	5.88	9.11	59.61
	100th	17.1	14.99	113.3

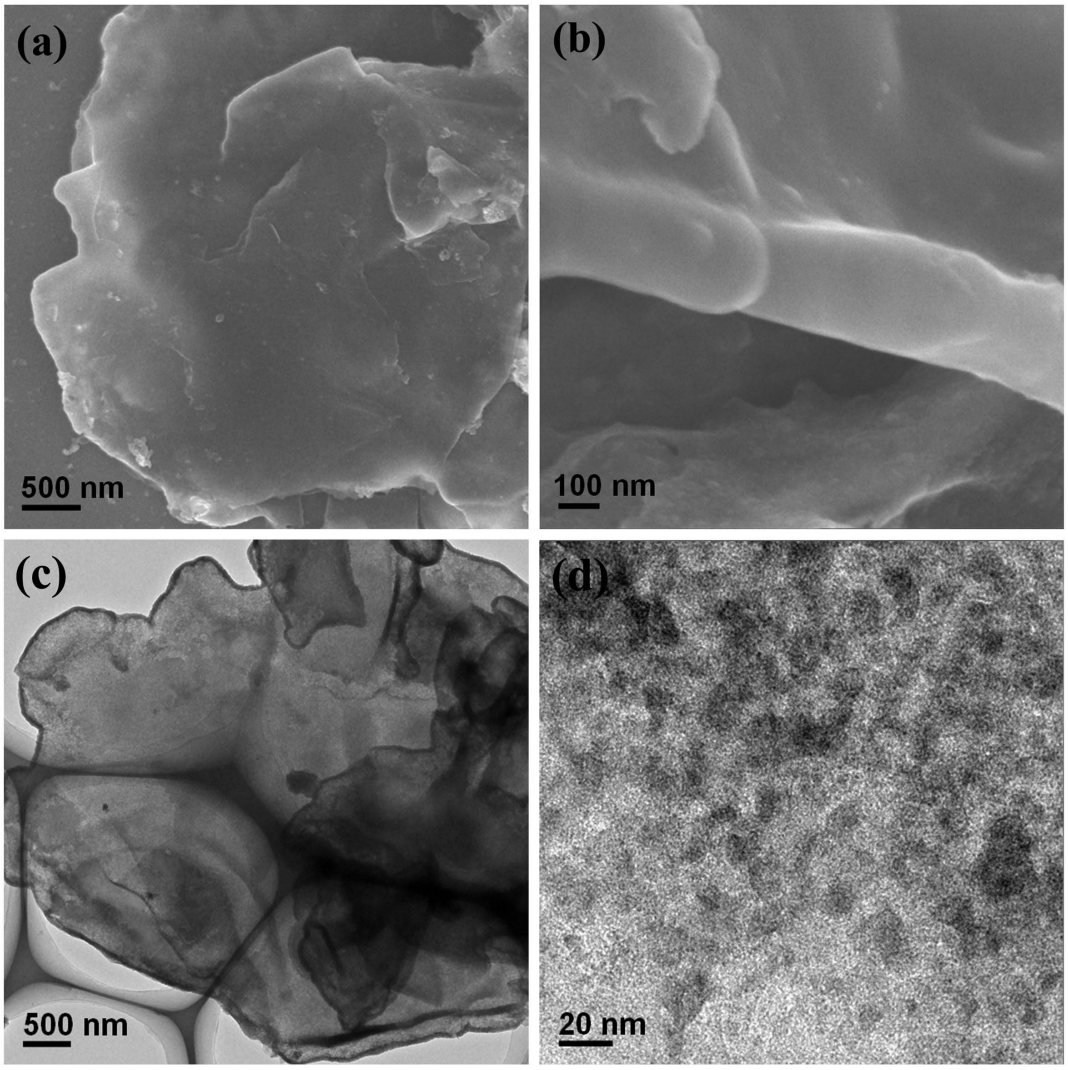

Fig. S20 (a-b) SEM and (c-d) TEM images of G@p-SnO_2@C electrode after 100 cycles, showing the excellent structure stability of this composite during cycles.